



HAL
open science

Light Control of Charge Transfer and Excitonic Transitions in a Carbon Nanotube/Porphyrin Hybrid
Yani Chen, Guy Royal, Emmanuel Flahaut, Saioa Cobo, Vincent Bouchiat, Laëtitia Marty, Nedjma Bendiab

► **To cite this version:**

Yani Chen, Guy Royal, Emmanuel Flahaut, Saioa Cobo, Vincent Bouchiat, et al.. Light Control of Charge Transfer and Excitonic Transitions in a Carbon Nanotube/Porphyrin Hybrid. *Advanced Materials*, 2017, 29 (18), pp.1605745. 10.1002/adma.201605745 . hal-01505016

HAL Id: hal-01505016

<https://hal.science/hal-01505016>

Submitted on 10 Dec 2020

HAL is a multi-disciplinary open access archive for the deposit and dissemination of scientific research documents, whether they are published or not. The documents may come from teaching and research institutions in France or abroad, or from public or private research centers.

L'archive ouverte pluridisciplinaire **HAL**, est destinée au dépôt et à la diffusion de documents scientifiques de niveau recherche, publiés ou non, émanant des établissements d'enseignement et de recherche français ou étrangers, des laboratoires publics ou privés.

Light control of charge transfer and excitonic transitions in a carbon nanotube/porphyrin hybrid

Yani Chen,[†] Guy Royal,[‡] Emmanuel Flahaut,[¶] Saioa Cobo,[‡] Vincent Bouchiat,[†]
Laëtitia Marty,[†] and Nedjma Bendiab^{*,†}

[†]*Institut Néel, Université Grenoble Alpes, BP 166, Grenoble Cedex 9, 38042, France*

[‡]*Univ. Grenoble Alpes, DCM UMR 5250, F-38000 Grenoble, France; CNRS, DCM UMR 5250, F-38000 Grenoble, France*

[¶]*CIRIMAT, UMR CNRS-UPS-INP N° 5085, Université Toulouse 3 Paul Sabatier, Bât. CIRIMAT, 118, route de Narbonne, 31062 Toulouse cedex 9, France*

E-mail: nedjma.bendiab@neel.cnrs.fr

Keywords: Nanotubes, Optoelectronics, Single electron tunneling, Raman enhancement, Porphyrins.

Abstract

Carbon nanotube-chromophore hybrids are promising building blocks in order to obtain a controlled electro-optical transduction effect at the single nano-object level. In this work, we observe a strong spectral selectivity of the electronic and the phononic response of our chromophore-coated single nanotube transistor for which standard photo-gating cannot account. We investigate how light irradiation strongly modifies the coupling between molecules and nanotube within the hybrid by means of combined Raman diffusion and electron transport measurements. Moreover, we observe a non-conventional Raman enhancement effect when light irradiation is on the absorption range of the grafted molecule. Finally, we show how the dynamics of single electron

tunneling in the device at low temperature is strongly modified by molecular photo-excitation. Both effects will be discussed in terms of photo-induced excitons coupled to electronic levels.

Low dimensional sp^2 carbon nanostructures such as graphene and nanotubes have emerged as ideal platforms for molecular electronics enabling new functional devices such as ultrasensitive molecule detectors, molecular scale logics and quantum devices.¹ In particular, nanotube ambipolar behavior along with direct bandgap allows their use for optoelectronics.² However, single wall nanotubes (SWNTs) are sensitive to any non specific and slight fluctuation in their environment, which directly alters their opto-electronic properties. Grafting chromophores onto nanotubes is an hybrid route towards specific functions for nanoelectronics. It is of great interest and challenging to reach the limit of hybrids at the single nanotube level. In this limit, the number of active molecules is limited by the 1D geometry and a single nano-object can be detected.³⁻¹⁰ In the particular case of optically active hybrids, Zinc(II) metalloporphyrins coating a SWNT network field effect transistor (FET) device was proposed for light harvesting.¹¹ Recent applications of porphyrin dyes for dye-sensitized solar cells have shown high yield in light energy harvesting.¹² However, only few studies have demonstrated efficient photo-induced charge transfer in nanotubes/porphyrins hybrid systems by using electrochemical methods,¹³ photoluminescence excitation experiments¹⁴ and absorption spectroscopy.¹⁵ These works highlight the importance of energy and/or charge transfers between molecules and nanotubes either in assembly of nanotubes or in isolated nanotubes in solution. Here we investigate how light excitation can be used to tune the signatures of the hybrids related to nanotube/chromophore coupling: the enhancement of the Raman signal from the so-called GERS effect^{16,17} and the onset of single charge trapping with molecular traps.¹⁸ These well-known effects should dramatically depend on light exposure in the case of chromophores, which has not been addressed yet.

To investigate the dependence of electronic and phononic response of a chromophore-coated single nanotube transistor under light irradiation, our approach consists in using com-

plementary Raman spectroscopy and electron transport measurements on the same samples. First, we will discuss how grafting chromophores on a single nanotube transistor induces a visible charge transfer in both phononic and electronic response. In a second part, we report on a strongly non conventional vibrational response under light irradiation of the hybrid at different wavelengths. Finally, we will address the possibility to control the dynamics of single charge trapping with light at low temperature.

The chromophore used here is a porphyrin moiety metallated with a Zinc(II) ion in its center named as Zinc(II)-meso-tetraphenylporphyrin (see Figure 1(a), TPPZn in the following).

Porphyrins provide an extremely versatile synthetic platform for a variety of applications.¹⁹ Their optical properties are very interesting for energy transfer with molecular control^{14,20} and for potential applications in optoelectronics.²¹ The absorption spectrum of TPPZn in toluene exhibits an intense Soret band at 422 nm and a main Q band at 549 nm (see Figure 1(a)).^{22,23} This zinc-based molecule was demonstrated to provide photo-gating on nanowires and nanotubes^{11,24} and furthermore presents the advantage of being reversibly charged by using light excitation in an easily accessible visible range. The Raman spectrum of TPPZn powder at 532 nm excitation line presents a huge luminescence which does not allow us to measure the Raman fingerprint of the molecule (not shown) whereas the one at 488 nm presents the two main molecular modes at 1356 cm^{-1} and 1547 cm^{-1} corresponding to the C-C bond vibration and to a combined modes of carbon-carbon vibration and carbon-azote vibration²⁵ (Figure 1(b)).

This study was conducted on 16 double wall carbon nanotube FETs (CNFETs) which exhibit similar behavior under grafting and light irradiation. First step consists in characterizing the double wall nanotube (DWNT) electronic nature by cross-correlating Raman spectra and gate transfer characteristics. On Figure 1(b), one Radial Breathing Like Mode (RBLM) and the G Raman modes of an hybrid DWNT transistor are presented. Since resonance conditions were not completely fulfilled for all FETs, we focus, in the following, on a

typically resonant transistor for the sake of clarity in the observed effect. In the G band region, a main peak around 1589 cm^{-1} is observed along with a metallic-like Breit-Wigner-Fano (BWF) shoulder. The G band shape and the position of the RBLM are compatible with an inner semi-conducting tube and an outer metallic tube (see supplementary information for details). After acquiring the Raman spectra and I-V curves of the pristine device, a solution of TPPZn in tetrahydrofuran (THF) was drop-casted onto DWNT transistors which were then rinsed with THF and dried under nitrogen. AFM characterization (see Supplementary Information) shows that molecules tend to cluster onto the nanotube (cluster size of about 30 nm). At 532 nm, we observe the presence of the TPPZn fingerprint superimposed onto the nanotube one, whereas no peak was observed in the molecule powder at this wavelength. This quenching of TPPZn luminescence by nanotube at this wavelength allow us to detect the molecular Raman modes. It's also an indication of the effective coupling between these two moieties.^{7,26,27} Moreover, after the deposition, the nanotubes modes are enhanced by a factor 4 to 7 in intensity and their frequency are downshifted by 3 cm^{-1} for the G mode (see Figure 1(b)). These signatures indicate a charge transfer between molecules and nanotubes after grafting. Furthermore, such intensity enhancement and luminescence quenching are a signature of chemical enhancement from charge transfer and/or dipolar effect between the nanotube and the molecules.^{17,26} Regarding transistor operation at room temperature (see Supplementary Information), the hybrid CNFET exhibits a p-type field effect characteristics which is in agreement with the G band frequency downshift. Moreover, the nanotube hybrid transistor shows a relatively low conductance in the off state (1.3 nS), and an on-to-off ratio of 65, in agreement with previous reports of porphyrin coated SWNT FETs, which was explained as the result of the addition of charged scattering sites distributed randomly along the nanotube.⁷

These features are typical of nanotube/molecular hybrids; we will focus in the following on the evolution of these electronic and phononic features under light exposure.

Figure 2 shows the influence of light illumination on a typical CNFET. We compare the

vibrational and electrical responses of this CNFET under light irradiation with wavelength range outside the absorption bands of the molecule about 470-480 nm and with a wavelength in the absorption range of the molecule about 550-560 nm. Figure 2 (a) and (b) shows that the I-V curve is not significantly changed under illumination at 475 nm whereas a shift of about +1.3 V is observed for an illumination at 555 nm. When shining green light over the sample, 13 FETs (81%) show positive shifts of the threshold voltage (with a mean shift of +3V) corresponding to holes transfer from the molecule to the nanotube under light illumination. Actually, TPPZn molecules turn negatively charged upon irradiation and act as an additional gate onto the nanotube. Considering the molecule are in close vicinity to the nanotube,²² this photo-gating is efficient.

This spectral selectivity is also observed on the phononic response. Actually, we record Raman spectra of the devices under white light illumination for both 488 nm and 532 nm Raman laser excitations (see Figure 3). At 532 nm excitation line, only a global enhancement is observed (Figure 2a) whereas at 488nm, a non conventional Raman behavior is observed. In fact, at 532 nm, a slight reversible frequency upshift of the G band components is measured from the dark to the light on state (see supplementary information for the fitting details), allowing us to conclude that only a small charge transfer occurs. Another general feature that appears under light illumination is the broadening of the G⁻ peak and an increase of the background. These effects are compatible with a weak charge transfer and a partial luminescence from molecules respectively.

At 488 nm, the enhancement of the G modes is far different from the 532 nm case. The G mode region exhibits dramatic changes: under light exposure only, two large peaks turn out to be visible, one of them matching the dark state G mode with an upshift of 1 cm⁻¹ and an intensity twice higher, whereas the most intense one at 1587 cm⁻¹ was barely visible in the dark state. When the light is turned off, the new observed intense peak vanishes, while the other mode remains, still shifted by 1 cm⁻¹ and reduced in intensity. Different explanations can be proposed for such a photo-induced signature. The first one is that the

nanotube is not fully covered with the molecules, thus some parts of it could sense the optical gating from the molecules whereas some remain unchanged. This would lead to a spectrum featuring superimposed peaks from the two portions, coupled and not to the molecules. In such case we would expect to observe superimposed features also in the dark state which is not the case. Moreover light excitation brings the molecules in a new redox state which is stable for a few hours at room temperature. Such a state can transfer the photo-generated charges to the nanotube as visible by the shift of the G mode. This shift is compatible with surface charges on the nanotube induced by the molecules but it cannot account for the rise of a new peak when light is on.

We rather consider that under light irradiation, the Soret and Q states of the porphyrin are populated so that energy is transferred from these molecular states to the nanotube excitonic state as already observed in SWNT photoluminescence experiments.²⁸ Excitonic states can have a major influence on the Raman intensity: if the Raman diffusion process involves a transition between a vibronic state of the nanotube that is close to an excitonic one, the coupling between these states allows the enhancement of the Raman cross section as described by Islam *et al.*²⁹ They observed such an enhancement for a phonon mode of CdSe quantum dots coupled to pyridine molecules where the laser excitation energy is in resonance with a charge transfer state and an excitonic state of the hybrid. In our case, we thus attribute the enhancement of one intrinsic mode of the nanotube G band to a Raman process promoted by charge transfer resonance and an excitonic resonance in our hybrid device. Since the two optical phonons G^+ and G^- present different symmetries, they will be enhanced differently depending on the dipolar influence of the excitons in the system. Regarding the different enhancement factors between the Raman spectra at 532 nm and at 488 nm, only laser line at 488 nm exhibits a dramatic enhancement of optical phonons, while 532 nm line is resonant with the nanotube (RBLM modes are visible meaning the laser matches an electronic transition) but do not show so strong enhancement. These two observations strongly suggest that this enhancement arises from a resonance of the 488 nm

line with the molecular charged state (after illumination) and with the excitonic state of the nanotube. Indeed, energy separation between the two laser lines (210 meV) is compatible with the energy of excitons in a nanotube.

Interestingly, the redox state reached by the molecule under light irradiation is stable for hours after illumination whereas the non conventional Raman effect disappears as the light is turned off. In order to get more insights into the underlying dynamics of these phenomena, we recorded the time evolution of the electrical and vibrational response of the hybrid device. Figure 4 shows the resistance of an hybrid CNFET during a dark/light-on/light-off cycle as shown on the timeline. The gate voltage is set at a constant value of 22 V so that the CNFET is in the threshold regime and not fully saturated in order to gain electrostatic field sensitivity. When switching on the light, we observe a resistance decrease from 20 to 17 k Ω (-15%) which, according to the transfer characteristics shown in Figure 2, corresponds to an effective p-doping. The time needed to reach a new steady state is of about 100 s. When switching off the light after 80 s, we observe no significant change in the resistance of the device. We tested over 16 samples, among which only one went back to the previous state after 2 days in ambient condition. However, by applying a gate voltage about -40 V on the backgate, we observe that within 150 s the resistance reaches a new steady state. In order to avoid the influence of the hysteresis, we then apply +30 V backgate voltage. When the backgate is tuned from 30 V to 22 V, the resistance goes back to 22 k Ω , which is similar (-15%) to the dark state of the CNFET (not shown). Thus, we can use the back-gate voltage to control and reset the illumination effect on the molecule in the hybrid in order to perform repeated operation of the optical switching of the device.

Similar behavior is observed in the vibrational response in burst mode Raman spectroscopy: a short accumulation time (1s) was used so as to record one spectrum every five seconds, and cycles of 100 s illumination followed by off states of 100 s were applied. For the first cycle, there is a clear doubling of the RBM intensity (x 2) when switching the light on, with a constant time of about 50 s, followed at the switching off by a decrease to a lower

value than finally to the dark state (-25%) with a constant time of about 60 s. Almost the same behavior is observed on the G band (a lowering of -22% with a time constant around 40 s, not shown). Similar measurements were performed for non functionalized devices which showed no effect at all.

Both Raman and transport measurements show that two different dynamics come into play. First, a relatively fast process with a constant time of 50 s reveals the weak capacitive coupling between the nanotube and the molecules. The second process involves long characteristics time constants up to hours corresponding to the relaxation time of charges trapped around the nanotube either in the substrate or in molecules around.

From room temperature experiments we conclude that the dramatic enhancement of the phonon signature of the hybrid is due to the possibility of resonantly transferred excitons from the charged state of porphyrins to the nanotube under light exposure. Furthermore, the persistence of the light induced doping is strongly dependent on charge trapping in the nanotube vicinity. Charge trapping in nanotube transistors is related to adsorbates, defects or trapping sites in the oxide layer or at interfaces and is known to strongly modify effective doping.³⁰⁻³³ Charge trapping is thermally activated, in order to get insights into trapping mechanisms, we record single charge trapping/detrapping in the nanotube vicinity at low temperature depending on the light irradiation.

At low temperature (10K), the transfer characteristics is similar to that observed at room temperature but exhibits additional features superimposed on the regular field effect response. These features are hysteretic conductance steps regularly spaced both in gate voltage and in the logarithm of the conductivity (Figure 5(a)). This behavior is assigned to single charge transfer between a trap and the nanotube as already observed in single electron memories¹⁸ and CNFETs decorated with nanoparticles.^{3,6} In the hybrid system, single charge tunneling between molecular cluster and nanotube, the latter being also a single charge electrometer. Considering the nanometer range of the nanotube diameter, electric field lines are concentrated at the nanotube surface which promote charge tunneling with

the environment and detection through field effect of the transistor. Such features are not observed on non-functionalized nanotubes and are assigned to the presence of the deposited molecules. From the voltage change between two steps, one can infer the capacitance C_T between the trap T and the nanotube channel as:

$$C_T = \frac{e}{\Delta V_G} \quad (1)$$

where $\Delta V_G = 0.56$ V which gives $C_T = 0.3$ aF. AFM performed on our devices shows that the molecular grains are larger than the nanotube diameter and about 30 nm (see Supplementary Information), so we can approximate C_T with a simple cylinder-plane capacitance model:

$$C_T = \frac{2\pi\epsilon_0\epsilon_r d_T}{\ln\left(\frac{h + \sqrt{h^2 - d_{NT}^2}}{d_{NT}}\right)} \quad (2)$$

where d_{NT} is the nanotube diameter (2 nm), d_T is the trap size and h is the tunneling distance between the trap and the nanotube. We then obtain a distance of about 30 nm which allows to observe signatures of charge tunneling. Since the steps are regularly spaced in gate voltage, we conclude that the associated trap is not a single molecule which would rather exhibit molecular orbital spectrum. We thus attribute these regular peaks to a cluster of molecules in the Coulomb blockade regime. Furthermore, the presence of hysteresis between the up and down ramps of gate voltage is a signature of irreversibility in the charge tunneling (Figure 5(a)). Such irreversibility cannot occur in a single tunneling junction, but requires junctions in series implementing a so-called multiple tunneling junction (MTJ).¹⁸ In such junctions, charges tunnel one by one along a series of potential wells which could be due in our case to tunneling from one molecule to another within the cluster before tunneling to the nanotube.

When exposing the device to light illumination, the power is low on the sample to prevent heating. For red light illumination (Figure 5 b), we observe very little changes on the

transfer characteristics: steps are still visible with the same spacing and shifted by only 0.1 V. Neither smoothing nor resistance change which discard any eventual heating from the light. Dramatic changes occur when using a blue filter including the absorption range of the molecule. First we observe a global shift of the transfer characteristics by +1,5 V corresponding to an effective p-doping similar to the room temperature case. Moreover, we still detect quantized features which are regularly spaced with the same gate steps as without light, meaning that the trap self capacitance is still the same as without light. We attribute these features to the single charge transfers from the same molecular trap observed without light. This result is similar to what has been observed in porphyrins embedded in silica:³⁴ optical switching of tunneling effect was performed in molecule-based tunneling junctions. However this group observed a similar global shift at any wavelength which discarded the absorption by the molecules. In our case, the occurrence of a global shift for a wavelength matching the absorption peak of the molecule shows that the molecular optical transition is involved in the optical switching process. Furthermore, the most intriguing modification we observe, is the shape of these features which, from a staircase-like in darkness, turn to sharp peaks under blue illumination. If heating was involved, such features would have turned even less sharp. This is associated with a modification of the hysteresis in the trapping-detrapping event: when extracting the hysteresis area for the first step, we obtain an area $A_{dark} = 3.4 \cdot 10^{-6}$ S.V while under blue light exposure $A_{blue} = 1.6 \cdot 10^{-6}$ S.V which corresponds to a reduction of the hysteresis of 53%. According to Nakazato *et al.*,¹⁸ this area is a function of the trap charging energy, the temperature and the ratio v_s/v_{s0} where v_s is the gate voltage sweep rate and $v_{s0} = e/\tau C_T$ is characteristic of the MTJ and provides a time constant τ related to the charge tunneling dynamics. In our experiment, temperature and gate sweep rate are kept constant. We observe an overall shift of the characteristics upon blue light but the quantized steps exhibit same spacing as in the dark state. This spacing is directly proportional to the charging energy which we conclude to be constant upon illumination. From Nakazato's model, we conclude that the hysteresis area change is then directly due to a

modification of the time constant τ , pointing out to a modification in the dynamics of charge transfer through the MTJ, which is consistent with the work of Holloway *et al.*³⁵ Upon light exposure, the molecules involved in the MTJ turn excited which modifies the potential profile of the multiple barriers involved in the charge transfer to the nanotube. Indeed, Gruneis *et al.* have observed sharp features in the case of a trap being very well coupled to a nanotube.⁶ In our case, we conclude that from a weak nanotube-trap coupling in darkness, light allows optical switching of the MTJ into a strong coupling regime. The change in the coupling is difficult to quantify since we do not have information about the structure of the MTJ. Still since the hysteresis area is divided only by a factor two, we can conclude that the coupling is moderately tuned by light. This modification is though sufficient to observe modification of quantized steps into peaks related to the change of dynamics.

In summary, we demonstrate in this work the possibility to get a light-activated transistor based on a chromophore-coated single nanotube hybrids acting down to the single charge transfer limit at low temperature. We have shown that beyond charge transfer, photo-gating of hybrid nanotube/chromophore goes along with an unusual Raman signal enhancement for laser excitation energies which match the chromophore absorption range. This photo-generated Raman enhancement is a consequence of the energy transfer between the charged state of the molecule (after light absorption) and the excitonic state of the nanotube which leads to a renormalization of the Raman cross section. Both transport and Raman signals exhibit such spectral dependence.

Moreover, at low temperature, light exposure induces optical switching of the charge tunneling with a spectral dependence related to the molecule absorption spectrum. Furthermore, we also demonstrate the light action on kinetics in this carbon-nanotube-based single electron memories. The control of single charge tunneling with light is a novel aspect that will be further exploit with a better control of the chromophore nanotube coating.

Acknowledgement

The authors wish to thank B. Soula, E. Anglaret, V. Jourdain, M. Holzinger and R. Martel for fruitful discussions, V. Reita, D. Jegouso, T. Crozes for technical support. This work is supported by TRICO ANR, LANEF program (Cryoptics) and the Chinese Scholarship Council.

Experimental

Fabrication of the devices. A powder of catalytic-CVD double wall carbon nanotubes³⁶ is dispersed by ultrasonics in 1,2-dichloroethane (DCE) by mild sonication. About 20 μL of the suspension was deposited onto a patterned SiO_2/Si wafer by spin-coating. After deposition, DWNTs were located by low voltage scanning electron microscopy (SEM) to design 50 nm thick Pd electrodes by e-beam lithography. The lengths of the DWNTs are between 1 and 2 μm . **Characterization of the hybrids.** Absorption spectra are recorded using a VIS/NIR Lambda 900 spectrometer. Raman measurements were performed by using a confocal Witec alpha 500 and a T64000 Jobin Yvon spectrometer. In Witec spectrometer, the elastically scattered light from the sample is filtered out by a Notch filter, while the inelastically scattered light is collected and sent to a spectrometer with resolution less than 1 cm^{-1} . A typical Raman spectrum is acquired in 1-10 s. To avoid laser heating, laser power is kept below 0.5 $\text{mW}\cdot\mu\text{m}^{-2}$. Regarding the Raman spectra at 488 nm, the inelastic light was measured in the back-scattering configuration on a triple subtractive Jobin-Yvon T64000 micro-spectrometer in the same experimental conditions as on the Witec spectrometer. Room temperature transistor characteristics were obtained with a vacuum Desert Cryogenics probe station using two beryllium-copper probes. Transfer characteristics (Ids, Vg) curves were acquired in a current-biased lock-in configuration using a Stanford Research 830 lock-in amplifier. The transistor characteristics of the device were measured by applying a 50 nA drain-source current while sweeping the gate voltage between ± 30 V. Light

illumination of the device was performed by using an X-Cite 120Q excitation white light source with a constant power of about 100 W and different color filters (see Supp.Info). The low temperature transport measurements were performed thanks to a Janis optical cryostat down to 10 K.

References

- (1) Charlier, J.-C.; Roche, S. *Reviews of Modern Physics* **2007**, *79*, 677–732.
- (2) Avouris, P.; Freitag, M.; Perebeinos, V. *Nature Photonics* **2008**, *2*, 341–350.
- (3) Marty, L.; Bonnot, A.-M.; Bonhomme, A.; Iaia, A.; Naud, C.; André, E.; Bouchiat, V. *Small* **2006**, *2*, 110–5.
- (4) Charlie Johnson, A. T.; Staii, C.; Chen, M.; Khamis, S.; Johnson, R.; Klein, M. L.; Gelperin, A. *Physica Status Solidi (B) Basic Research* **2006**, *243*, 3252–3256.
- (5) Borghetti, J.; Derycke, V.; Lenfant, S.; Chenevier, P.; Filoramo, A.; Goffman, M.; Vuillaume, D.; Bourgoin, J.-P. *Advanced Materials* **2006**, *18*, 2535–2540.
- (6) Gruneis, A.; Esplandiu, M. J.; Garcia-Sanchez, D.; Bachtold, A. *Nano Letters* **2007**, *7*, 3766–3769.
- (7) Bogani, L.; Danieli, C.; Biavardi, E.; Bendiab, N.; Barra, A.-L.; Dalcanale, E.; Wernsdorfer, W.; Cornia, A. *Angewandte Chemie Int. Ed.* **2009**, *48*, 746–50.
- (8) Urdampilleta, M.; Klyatskaya, S.; Cleuziou, J.-P.; Ruben, M.; Wernsdorfer, W. *Nature Materials* **2011**, *10*, 502–6.
- (9) Bouilly, D.; Cabana, J.; Meunier, F.; Desjardins-Carrière, M.; Lapointe, F.; Gagnon, P.; Larouche, F. L.; Adam, E.; Paillet, M.; Martel, R. *ACS Nano* **2011**, *5*, 4927–4934.

- (10) Ganzhorn, M.; Klyatskaya, S.; Ruben, M.; Wernsdorfer, W. *Nature Nanotechnology* **2013**, *8*, 165–9.
- (11) Hecht, D. S.; Ramirez, R. J.; Briman, M.; Artukovic, E.; Chichak, K. S.; Stoddart, J. F.; Grüner, G. *Nano Letters* **2006**, *6*, 2031–2036.
- (12) Yella, A.; Lee, H.-W.; Tsao, H. N.; Yi, C.; Chandiran, A. K.; Nazeeruddin, M. K.; Diau, E. W.-G.; Yeh, C.-Y.; Zakeeruddin, S. M.; Grätzel, M. *Science* **2011**, *334*, 629–634.
- (13) Chitta, R.; Sandanayaka, A. S.; Schumacher, A. L.; D'Souza, L.; Araki, Y.; Ito, O.; D'Souza, F. *The Journal of Physical Chemistry C* **2007**, *111*, 6947–6955.
- (14) Roquelet, C.; Garrot, D.; Lauret, J.-S.; Voisin, C.; Alain-Rizzo, V.; Roussignol, P.; Delaire, J.; Deleporte, E. *Applied Physics Letters* **2010**, *97*, 141918.
- (15) Satake, A.; Miyajima, Y.; Kobuke, Y. *Chemistry of Materials* **2005**, *17*, 716–724.
- (16) Ling, X.; Xie, L.; Fang, Y.; Xu, H.; Zhang, H.; Kong, J.; Dresselhaus, M. S.; Zhang, J.; Liu, Z. *Nano Letters* **2010**, *10*, 553–561.
- (17) Huang, S.; Ling, X.; Liang, L.; Song, Y.; Fang, W.; Zhang, J.; Kong, J.; Meunier, V.; Dresselhaus, M. S. *Nano Letters* **2015**, *15*, 2892–2901, PMID: 25821897.
- (18) Nakazato, K.; Blaikie, R. J.; Ahmed, H. *Journal of Applied Physics* **1994**, *75*, 5123–5134.
- (19) Wöhrle, D.; Schnurpfeil, G. *The Porphyrin Handbook*; 2003; Vol. 11; pp 177–246.
- (20) Magadur, G.; Lauret, J.-S.; Charron, G.; Bouanis, F.; Norman, E.; Huc, V.; Cojocaru, C.-S.; Gómez-Coca, S.; Ruiz, E.; Mallah, T. *Journal of the American Chemical Society* **2012**, *134*, 7896–901.

- (21) Suslick, K. S.; Rakow, N. a.; Kosal, M. E.; Chou, J. H. *Journal of Porphyrins and Phtalocyanines* **2000**, *4*, 407–413.
- (22) Correa, J.; Orellana, W. *Physical Review B* **2012**, *86*, 125417.
- (23) Vialla, F.; Roquelet, C.; Langlois, B.; Delpont, G.; Santos, S. M.; Deleporte, E.; Roussignol, P.; Delalande, C.; Voisin, C.; Lauret, J.-S. *Physical Review Letters* **2013**, *111*, 137402.
- (24) Winkelmann, C. B.; Ionica, I.; Chevalier, X.; Royal, G.; Bucher, C.; Bouchiat, V. *Nano Letters* **2007**, *7*, 1454–1458.
- (25) Jeong, D. H.; Yoon, M.-C.; Jang, S. M.; Kim, D.; Cho, D. W.; Yoshida, N.; Aratani, N.; Osuka, A. *The Journal of Physical Chemistry A* **2002**, *106*, 2359–2368.
- (26) Lopes, M.; Candini, A.; Urdampilleta, M.; Reserbat-Plantey, A.; Bellini, V.; Klyatskaya, S.; Marty, L.; Ruben, M.; Affronte, M.; Wernsdorfer, W.; Bendiab, N. *ACS Nano* **2010**, *4*, 7531–7537.
- (27) Andrada, D. M.; Vieira, H. S.; Oliveira, M. M.; Santos, A. P.; Yin, L.; Saito, R.; Pimenta, M. A.; Fantini, C.; Furtado, C. A. *Carbon* **2013**, *56*, 235–242.
- (28) Vialla, F.; Malic, E.; Langlois, B.; Chassagneux, Y.; Diederichs, C.; Deleporte, E.; Roussignol, P.; Lauret, J.-S.; Voisin, C. *Physical Review B* **2014**, *90*, 155401.
- (29) Islam, S. K.; Sohel, M. a.; Lombardi, J. R. *Journal of Physical Chemistry C* **2014**, *118*, 19415–19421.
- (30) Radosavljević, M.; Freitag, M.; Thadani, K. V.; Johnson, A. T. *Nano Letters* **2002**, *2*, 761–764.
- (31) Fuhrer, M. S.; Kim, B. M.; Dürkop, T.; Brintlinger, T. *Nano Letters* **2002**, *2*, 755–759.

- (32) Choi, W. B.; Chae, S.; Bae, E.; Lee, J.-W.; Cheong, B.-H.; Kim, J.-R.; Kim, J.-J. *Applied Physics Letters* **2003**, *82*, 275.
- (33) Aguirre, C. M.; Levesque, P. L.; Paillet, M.; Lapointe, F.; St-Antoine, B. C.; Desjardins, P.; Martel, R. *Advanced Materials* **2009**, *21*, 3087–3091.
- (34) Wakayama, Y.; Ogawa, K.; Kubota, T.; Suzuki, H.; Kamikado, T.; Mashiko, S. *Applied Physics Letters* **2004**, *85*, 329–331.
- (35) Holloway, G. W.; Song, Y.; Haapamaki, C. M.; LaPierre, R. R.; Baugh, J. *Journal of Applied Physics* **2013**, *113*, 024511.
- (36) Flahaut, E.; Bacsá, R.; Peigney, A.; Laurent, C. *Chemical Communications* **2003**, 1442–3.

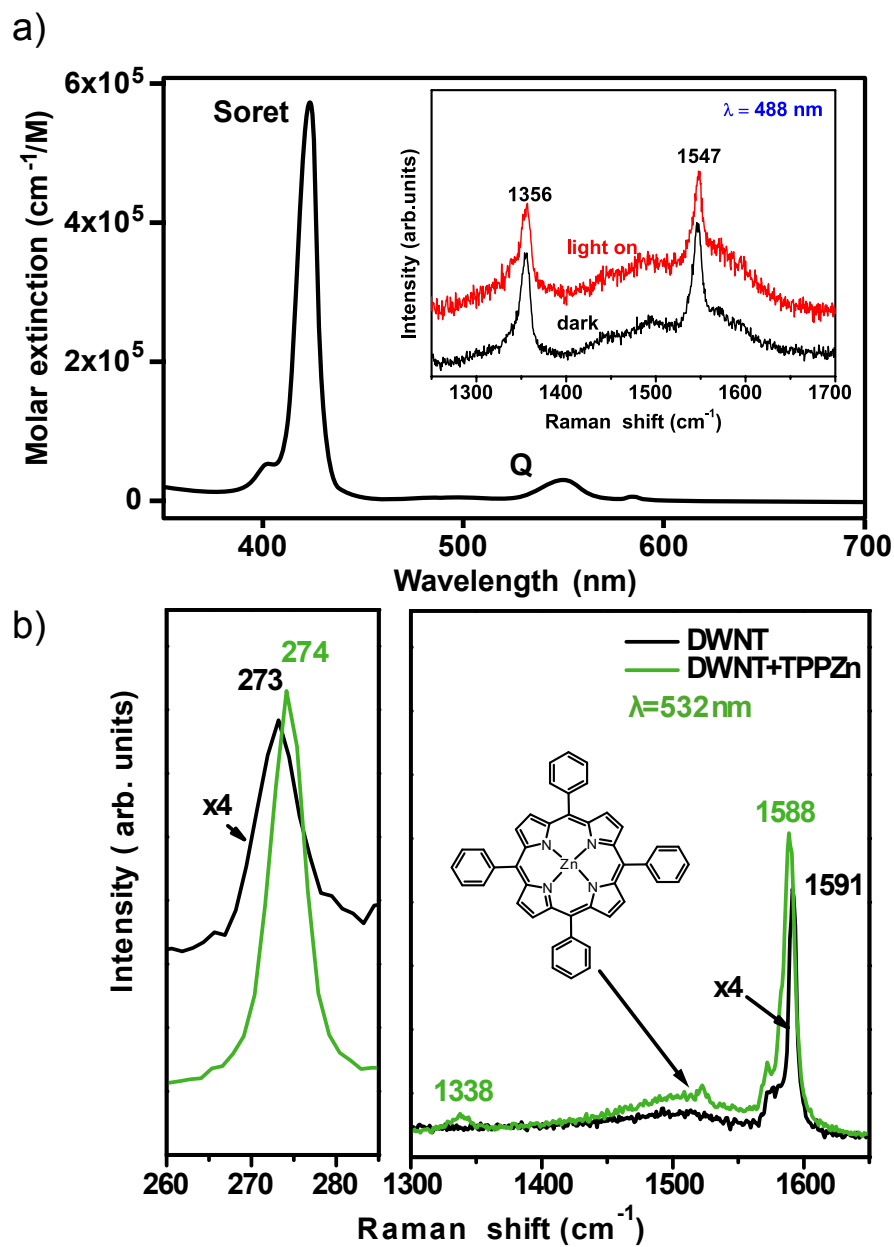


Figure 1: a) UV-visible absorption spectrum of TPPZn (inset: Raman spectrum of TPPZn powder with and without extra white light illumination. The Raman spectra are measured at excitation wavelengths of 488 nm), b) Raman spectrum of isolated DWNT-TPPZn hybrid transistor at 532 nm (inset: chemical structure of the zinc(II) metalloporphyrin derivative(TPPZn)).

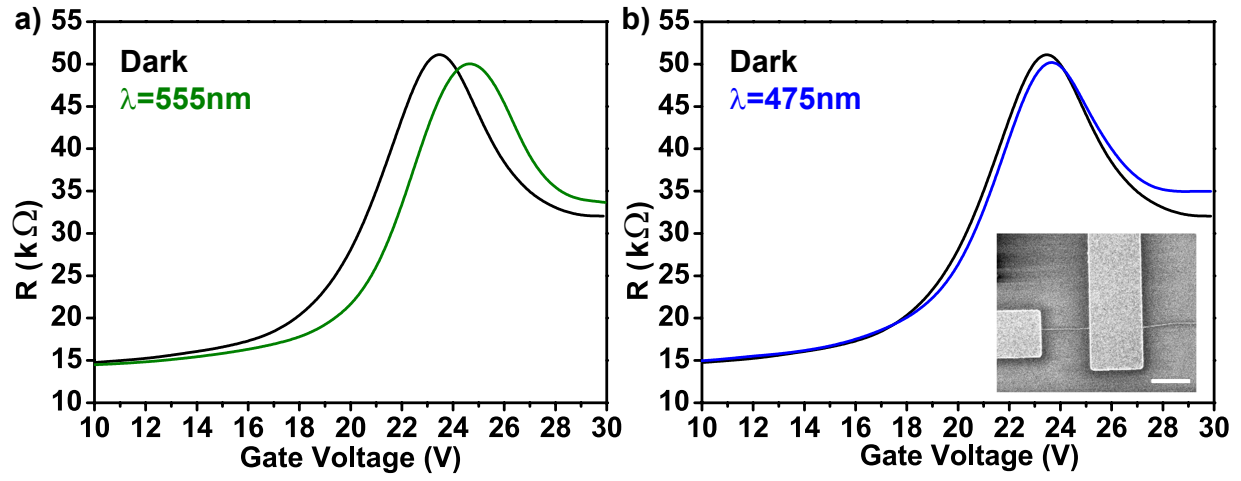


Figure 2: Light effect on hybrid CNFET. a) Transfer characteristics at room temperature in dark (black) and under 2 mW laser excitation at a) 475 nm (green) and b) 555 nm (blue) (inset: SEM image of an isolated DWNT transistor, scale bar is 1 μm).

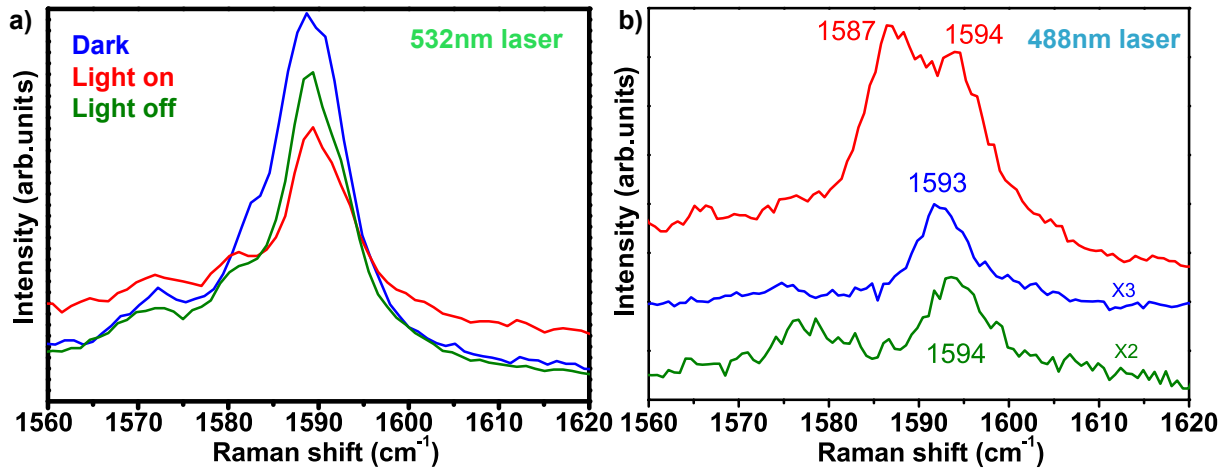


Figure 3: a) Raman spectra of DWNT/TPPZn under white light illumination measured at 532 nm. b) Raman spectra of DWNT/TPPZn under white light illumination measured at 488 nm. The blue spectra are before illumination (dark), the red ones are light on and the green ones correspond to back to dark.

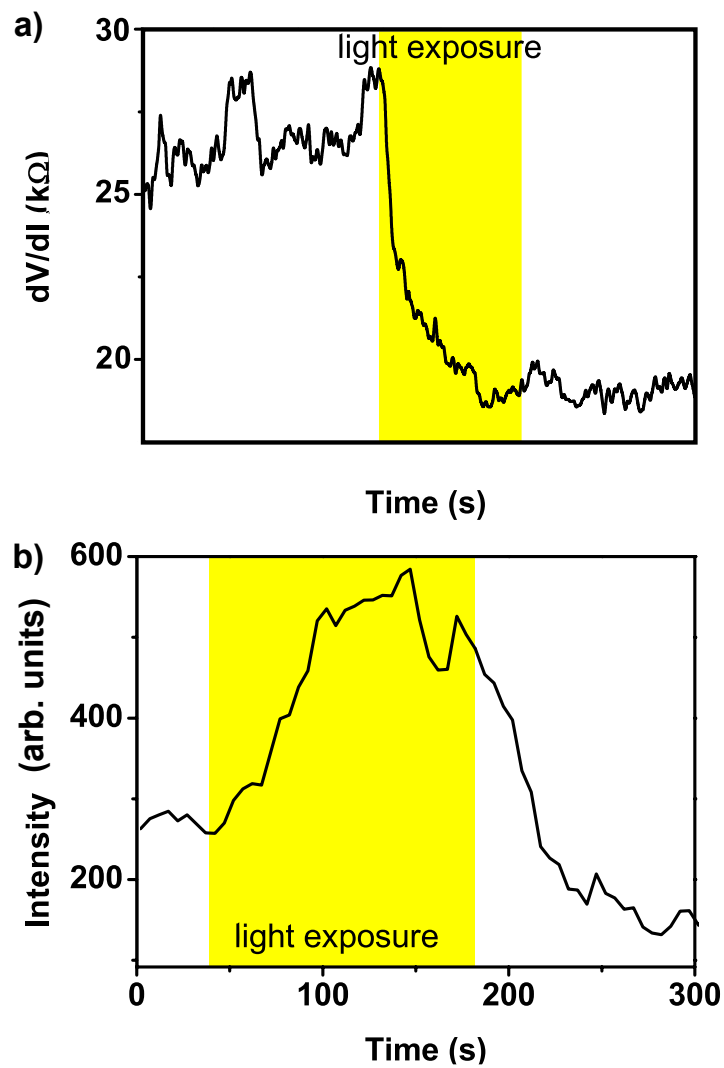


Figure 4: a) Differential resistance at $V_g = 22$ V and b) RBLM peak intensity evolution under a cycle of white light ON and OFF cycle.

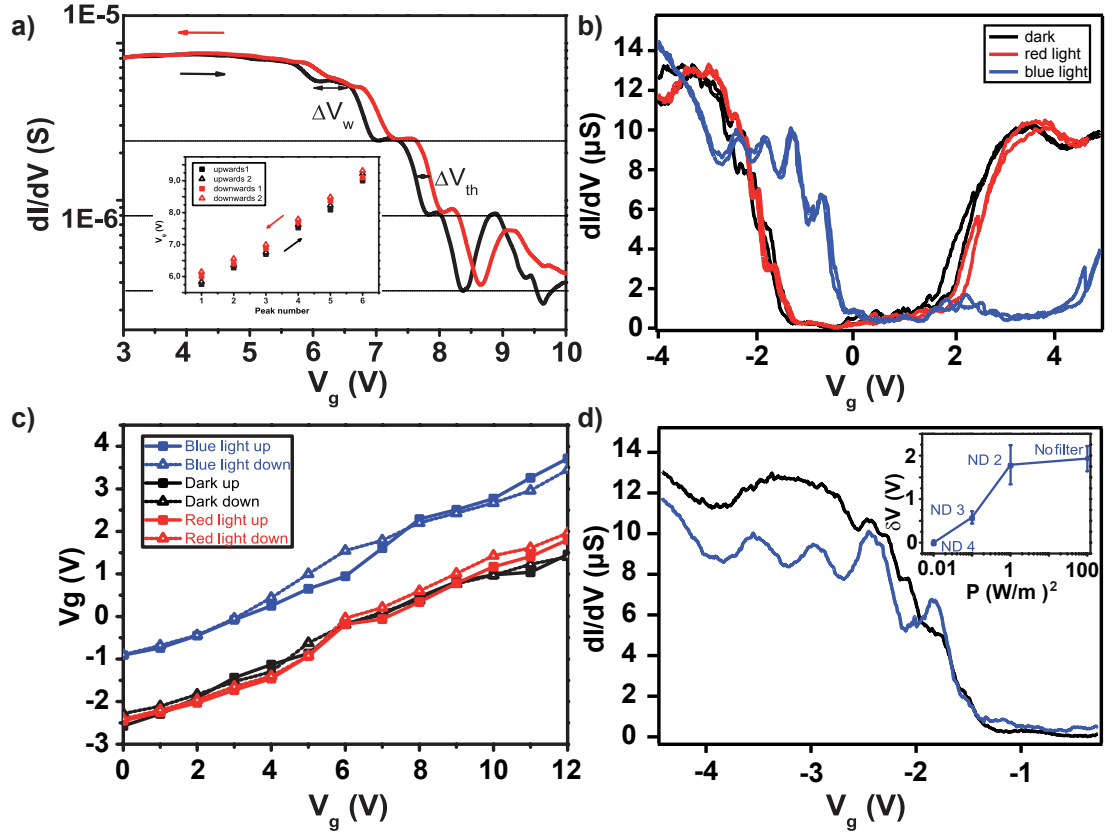


Figure 5: a) Transfer characteristics of DWNT/TPPZn hybrid transistor at 10 K. The curve is plotted at $V_{ds} = 1$ mV (AC) for opposite gate sweeps of ± 0.1 V/s (Inset shows the position of each step). b) Full hysteresis cycle of transfer characteristics of a DWNT/TPPZn hybrid transistor measured in dark (black curve), under red light illumination (red curve) and blue light (blue curve) at $V_{ds} = 1$ mV (AC). c) Gate voltage position of the steps shown in b). d) Same curves in dark and blue light for decreasing gate sweep and horizontally shifted for the sake of clarity (inset: Light power dependence of the observed gate shift obtained using neutral densities).